Soil & Tillage Research 174 (2017) 130–138

Contents lists available at ScienceDirect

Soil & Tillage Research

journal homepage: www.elsevier.com/locate/still

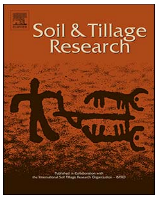

Cropland has higher soil carbon residence time than grassland in the subsurface layer on the Loess Plateau, China

Ding Guo[a], Jing Wang[a], Hua Fu[a,*], Haiyan Wen[a], Yiqi Luo[b]

[a] State Key Laboratory of Grassland Agro-Ecosystems, College of Pastoral Agriculture Science and Technology, Lanzhou University, Lanzhou 730020, China
[b] Department of Microbiology and Plant Biology, University of Oklahoma, Norman, OK 73019, USA

ARTICLE INFO

Keywords:
Carbon mineralization
Inverse analysis
Residence time

ABSTRACT

Carbon (C) residence time is one of the key factors that determine the capacity of C storage and the potential C loss in soil, but it has not been well quantified. Assessing C residence time is crucial for an improved understanding of terrestrial C dynamics. To investigate the responses of C residence time to land use, soil samples were collected from millet cropland (MC) and enclosed grassland (EG) on the Loess Platea, China. The soil samples were incubated at 25 °C for 182 days. A Bayesian inverse analysis was applied to evaluate the residence times of different C fractions based on the information contained in the time-series data from laboratory incubation. Our results showed that soil organic carbon (SOC) mineralization rates and the amount of SOC mineralized significantly was increased after the conversion of cropland into grassland due to the increase in labile C fraction. At the end of the incubation study, 2.1%–6.8% of the initial SOC was released. Our modeling analysis indicated that the sizes and pool of active C in EG were larger than those in MC. The residence times of slow C pool at the 10–30 cm layers were longer in MC (11.8–15.7 years) than those in EG (14.7–21.9 years). Our inverse analysis also directly reflected that the active C pool dominated C mineralization in the first 92 days, while the slow C pool was the largest contributor after 92 days. Conversion of cropland to grassland increases SOC decomposition, probably through increased active C pool resulted from higher litter input and no ploughing activities. The declined SOC in subsoil may be attributed to the short carbon residence times in grassland.

1. Introduction

As a key process of the ecosystem C and N cycling, the dynamics of soil organic carbon (SOC) regulates the supply of nutrient elements to plants, as well as CO_2 emissions into the atmosphere, which is associated with global warming (Davidson and Janssens, 2006; Ma et al., 2013; Mohanty et al., 2013; Wang et al., 2013). SOC is heterogeneous in nature and consists of different C pools with residence times ranging from days to millennia (Trumbore, 1997). Carbon residence times determine the capacity of C storage and potential C loss in soil (Luo et al., 2003), and are crucial parameters of C cycling model (Zhang et al., 2010; Zhou et al., 2012). Understanding the turnover times of different C pools would provide us with insight into future SOC dynamics, as well as global C cycling and climate change (Chen et al., 2013; Friend et al., 2014).

In most conventional models of C cycling, SOC has been simply divided into at least three pools with different residence times: an active pool with residence times of a few days to a few months; a slow pool with residence times of a few years; and a passive pool with the residence times of hundreds to thousands years (Parton et al., 1988; Xu et al., 2006). In the CENTURY model, for example, SOC is partitioned into three pools that are classified as an active fraction of soil C with turnover time 1–5 years, a slow SOC fraction with turnover time 20–40 years, and s passive SOC fraction with turnover time 200–1500 years (Parton et al., 1987). Several methods have been used to determine C residence times, such as a C balance method that calculates the ratios of each C pool stock divided by the corresponding flux (Vogt et al., 1996), radiocarbon (Fröberg et al., 2011; Saggar et al., 1996) and stable isotope techniques (Derrien and Amelung, 2011; Richards et al., 2007). However, these method had their limitations. For example, a C balance method is simple and easy to use, but not all C pool stock and the corresponding flux can be measured (Vogt et al., 1996). Soil radiocarbon methods usually overestimate residence times of labile C factions due to the failure of considering the heterogeneity of SOC (Trumbore, 2000). The soil stable isotope method is only suitable to estimate C residence time for ecosystems with different isotope signatures of source components (Derrien and Amelung, 2011; Richards et al., 2007). Because of the uncertainties of estimating residence times

---

[*] Corresponding author at: 768, Jiayuguan West Road, Lanzhou, Gansu, 730020, China.
E-mail address: lzufuhua@l26.com (H. Fu).

http://dx.doi.org/10.1016/j.still.2017.07.003
Received 7 March 2017; Received in revised form 20 June 2017; Accepted 2 July 2017

of different C pools, there are great difficulties in understanding terrestrial C dynamics to make policies to mitigate climate change (Friend et al., 2014; Zhang et al., 2010; Zhou et al., 2012). Thus it is important to accurately quantify residence times of different C pool for improved understanding of terrestrial C dynamics.

Data assimilation is an approach that could improve parameter estimation by fusing observed data into models and get new information from available data, which cannot be directly determined from experiments (Luo et al., 2009; Raupach et al., 2005). Among various data assimilation techniques, Bayesian inversion might be the most common approach for parameter estimation and has been successfully applied to estimate the residence times of different C pools (Zhang et al., 2010; Zhou et al., 2012). For example, Zhang et al. (2010) conducted Bayesian inversion to estimate the residence times of soil active, slow and passive pools by using six biometrics and soil datasets at three different forest ecosystems in eastern China.

The Loess Plateau is located at the northwest of China with a total area of 0.63 million km^2, and is known for its deep loess (Lu et al., 2004). Due to the population growth and pressure increases, vast areas of grassland have been converted to cropland due to the ever-increasing food demand (Li et al., 2010). Consequently, this region suffers from severe land degradation and serious soil erosion (Fu et al., 2005), which has also resulted in a reduced capacity for C sequestration (Chang et al., 2011). To solve those serious problems, the Chinese government launched some programmes to convert cropland to grassland, shrub and forest (Feng et al., 2013; Lü et al., 2012). Generally, conversion of cropland into grassland might lead to an increase in SOC derived from decreased carbon loss from soil erosion, increased organic matter inputs and reduced mineralization due to the removal of tillage (Chang et al., 2011; Feng et al., 2013). Our previous studies showed that SOC decreased in the subsurface layer after cropland was abandoned due to the downwards movement of surface soil organic matter (Guo et al., 2013; Li et al., 2008), whereas, the SOC storage within 1 m soil depth in millet cropland was 40% higher than that in enclosed grassland (Li et al., 2008), which has not been well explained.

Carbon influx and residence time are two crucial factors for determining C sequestration capacity (Luo et al., 2003). C inputs in soil are higher in grassland than that in cropland (Li et al., 2008). Therefore, we hypothesized that C residence times would be longer in cropland compared to those in grassland. In this study, we measured CO$_2$ evolution from laboratory incubation experiment to examine SOC decomposition in cropland and grassland. Then we applied Bayesian inverse analysis to estimate the sizes and residence times of different C pools based on information contained in incubation data.

2. Materials and methods

2.1. Site description

The study was conducted at the Semi-Arid Climate and Environment Observatory of Lanzhou University (35° 57′N, 104° 09′E, elevation 1966 m), with a continental semiarid climate. The mean annual precipitation is about 382 mm and the mean annual air temperature is 6.7 °C. The soil is classified as a Sierozem (inceptisols, USDA Soil Taxonomy).

The experiment consisted of two land use types: (1) millet cropland (MC) that had been under conventional tillage for at least 50 years, and (2) enclosed grassland (EG). Parts of cropland were abandoned for self-recovery and turned into grassland since 1986. The experimental sites were located at similar altitudes and slopes ($< 5°$) and shared a common bedrock, parent material (loess), and considered to be homogeneous. Soil physical, chemical, and biological properties were assumed to be initially similar in the two lands because they were managed as a single unit during the agricultural period (Lee and Jose, 2003). The texture of the surface soil (0–30 cm) is 14% sand, 76% silt and 10% clay in MC, and it is 16% sand, 75% silt and 9% clay in EG. The plants in cropland were *Solanum tuberosum* L. (potato), *Setaria italica* Beauv. (Millet) and *Linum usitatissimum* L. (Benni) in rotation. The dominated grasses were *Stipa bungeana* and *Artemisia frigida Willd.* Fertilizers that include organic manure (3000 kg dry matter ha^{-1}) and chemistry fertilizer (30 kg N ha^{-1} and 60 kg P$_2$O$_5$ ha^{-1}) were applied to cropland before sowing. The fertilization was the same for the three crops, and the organic manure was sheep manure (200 g C kg^{-1}). Instead of cutting, the whole crop (including the stubble) was harvested with little residue left in the field. The depth of tillage is about 10 cm. Three 50 × 50 m^2 plots for each land use type were randomly established in 2005, with the distance of over 50 m between them that assured independence of replicates.

2.2. Soil sampling and analysis

Soil samples were collected in May 2012. Two parallel 50 m transects, 17 m apart, were selected at each plot for soil sampling. Five soil columns were sampled at each transect at three soil depths (i.e. 0–10, 10–20 and 20–30 cm). The soil samples at each plot were mixed as one composite sample for the same depth. A subsample of fresh soil was sieved (< 2 mm) immediately after collection and stored in a refrigerator (4 °C) for laboratory incubation. The remaining soil samples were air-dried for pH, soil organic carbon (SOC), total nitrogen (TN), and light fraction of soil organic carbon (LF-SOC) analysis.

Soil pH was analyzed at a soil: water ratio of 1:2.5 suspension (w/v) with a pH meter. SOC was measured by the dichromate oxidation method (Nelson and Sommers, 1996) and TN by the Kjeldahl method (Bremner, 1996) (0.25 mm soil sample). The light fraction of soil organic carbon (LF-SOC) was determined according to the procedure of (Gregorich and Ellert, 1993). Briefly, 25 g air-dried soil was weighed into a centrifuge tube with 50 ml NaI solution (density = 1.7 g cm^{-3}). The tube was shaken for 60 min, and then centrifuged at 1000g for 15 min. The floating material was filtered using a vacuum filter unit with 0.45 μm Whatman filter paper, and the material retained on the filter paper was washed with 0.01 M CaCl$_2$ and distilled water, and then oven dried at 60 °C for 48 h, weighed, and measured for C content. In addition, soil bulk density (BD) was determined using metal rings of known volume (100 cm^3). Detailed site conditions are shown in Table 1.

Soil C mineralization was measured by determining the amount of

Table 1
The properties of experimental soil used for incubation study.

Treatment	Soil layer depth (cm)	BD (g cm^{-3})	pH	SOC (mg g^{-1})	TN (mg g^{-1})	LF-SOC (mg g^{-1})
millet cropland	0–10	1.05 ± 0.04b	8.38 ± 0.14a	7.33 ± 0.21b	0.87 ± 0.02b	0.74 ± 0.12b
	10–20	1.07 ± 0.06b	8.36 ± 0.03a	7.16 ± 0.41a	0.96 ± 0.03a	0.56 ± 0.17a
	20–30	1.14 ± 0.06a	8.34 ± 0.04b	9.64 ± 0.37a	1.14 ± 0.08a	0.30 ± 0.01a
enclosed grassland	0–10	1.18 ± 0.04a	8.43 ± 0.01a	8.75 ± 0.10a	1.02 ± 0.02a	1.67 ± 0.38a
	10–20	1.19 ± 0.04a	8.36 ± 0.04a	6.40 ± 0.60a	0.87 ± 0.04b	0.74 ± 0.13a
	20–30	1.20 ± 0.01a	8.57 ± 0.1a	6.01 ± 0.51b	0.77 ± 0.01b	0.36 ± 0.06a

Different letters mean significant differences between the two sites (independent sample *t* test, $P \le 0.05$, n = 3). BD: bulk density, SOC: soil organic carbon, TN: total nitrogen, LF-SOC: light fraction of soil organic carbon. Values are mean ± SD.

CO_2 evolved (Alef, 1995). Soil samples (equivalent to 100 g dry mass) with moisture adjusted to 60% water holding capacity (WHC) were placed in 1L frosted glass jars with lids. A plastic beaker containing 10 ml of 0.5 M NaOH to absorb CO_2 and a beaker of 10 ml of distill water (prevent soil drying) were placed in the glass jar. Meanwhile, controls (without soil samples) were also incubated incubators. The glass jars were placed at a constant temperature 25 °C for 182 days in RXZ-380 incubators (Ningbo Jiangnan Instrument Factory, zhejiang, China). On days 2, 4, 6, 9, 12, 16, 20, 27, 34, 48, 62, 92, 122, 152 and 182, CO_2-C evolved from soil was determined by titration with 0.1 M HCl. After the NaOH beaker was taken out, the glass jars were opened for 2 h to allow replenishment of O_2. The soil moisture was checked by weighting the glass jars and was adjusted with distilled water when necessary.

2.3. Model description and parameters

The model that we used in this study is a variation of the simple first-order kinetic model developed by Andren and Paustian (1987). The model has three carbon pools including active (A_1C), slow (A_2C) and passive (A_3C) SOC. The model can be represented by the following first-order kinetic equation:

$$R_t = \sum_{i=1}^{3} A_i C_{tot}\left(1 - e^{-k_i t}\right) \tag{1}$$

Where R_t is the cumulative C mineralization after time t (mg C g^{-1} soil). A_i (i = 1, 2, 3) describes the initial fraction of labile, slow and passive SOC (%), respectively, and $A_1 + A_2 + A_3 = 1$. C_{tot} is the initial SOC content (mg C g^{-1} soil). K_i is the decay rate of the ith pool (day^{-1}). In this study, partitioning coefficients (i.e., parameter A) and carbon turnover rates (i.e., parameter K) were the targets to be estimated. The inverses of the parameter K represent the mean of C residence times.

2.4. Parameter estimation

We used Bayesian probabilistic inversion approach (Xu et al., 2006) to estimate parameter A and K. Based on Bayes' theorem, the posterior probability density function (PDF) $p(\theta|Z)$ of parameters θ can be obtained from a prior knowledge of parameters (θ), represented by prior PDF $p(\theta)$, and the information contained in the soil incubation data, represented by likelihood function $p(Z|\theta)$.

$$p(\theta|Z) \propto p(Z|\theta)p(\theta) \tag{2}$$

To apply Bayes' theorem, we specified that the prior PDF $p(\theta)$ to be uniformly distribution over specific parameter ranges (Table 2). These ranges were estimated according to the methods employed by Sch & del et al. (2013), Weng et al. (2011), Zhou et al. (2010) and Xu et al. (2006). The likelihood function $p(Z|\theta)$ was expressed by Eq. (3) on the assumption that errors between observed and modeled data followed a Gaussian distributions.

$$p(Z|\theta) \propto \exp\left\{-\frac{1}{2\sigma^2}\sum_{t\in obs(Z_i)}[Z_i(t) - X_i(t)]\right\} \tag{3}$$

Where σ^2 is the standard deviation of the observed cumulative C mineralized, $Z(t)$ and $X(t)$ are the observed and modeled cumulative C mineralized.

The Metropolis-Hastings (M-H) algorithm, which was employed to construct posterior PDFs of parameters, is a Markov chain Monte Carlo (MCMC) technique revealing high-dimensional PDFs of random variables via a sampling procedure (Hastings, 1970; Metropolis et al., 1953). The details of this algorithm was described by Xu et al. (2006). We ran the M-H algorithm by repeating two steps: a proposing step and a moving step. In each proposal step, the algorithm generates a new parameter θ^{new} on the basis of the previously accepted parameter θ^{old} with a proposal distribution $p(\theta^{new}|\theta^{old})$ (Eq. (4)).

$$\theta^{new} = \theta^{old} + r(\theta_{\max} - \theta_{\min})/D \tag{4}$$

Where θ_{max} *and* $\theta_{\text{ min}}$ are the maximum and minimum parameter values in the prior range. r is a random variable taken from a uniform distribution between −0.5 and +0.5. D controls the proposing step size and was set to 5 in this study. In each moving step, parameter θ^{new} is tested against the Metropolis criterion to examine if it should be accepted or rejected (Eq. (5)).

$$p(\theta^{old}, \theta^{new}) = \min\left\{1, \frac{p(Z|\theta^{new})}{p(Z|\theta^{old})}\right\} \tag{5}$$

Gelman-Rubin (G-R) diagnostic method was used to examine convergence of MCMC simulation. Five parallel chains were run by starting with different initial parameter values. When the within-run variation was roughly equal to the between-run variation, the simulated Markov chain has reached convergence (Gelman and Rubin, 1992).

Histograms were constructed from the series of samples to display distributions of parameters in the parameter space. Maximum likelihood estimators (MLE) were calculated by observing the parameter values corresponding to the peaks of marginal distributions. Means of parameters (θ), were estimated by

$$E(\theta_i) = \frac{1}{f}\sum_{n=1}^{f} \theta_i^{(f)} \tag{6}$$

where f is the number of samples given by the M-H algorithm, and i = 1, 2,…5.

2.5. Statistical analysis

All statistical analyzes were conducted with SPSS 11.5 for Windows (SPSS, Inc., Chicago, IL, USA). The independent t-test was employed to compare soil pH, BD, SOC, TN, LF-SOC, and carbon mineralization

Table 2
prior ranges and maximum likelihood estimators (MLE) of parameters for the C dynamics model.

parameters	Lower limit	Upper limit	$MLE_{0-10\ cm}$		$MLE_{10-20\ cm}$		$MLE_{20-30\ cm}$	
			MC	EG	MC	EG	MC	EG
A_1 (%)	0	10	2.8	5.17	2.59	4.25	0.99	1.85
A_2 (%)	30	80	50.4^a	49.7^a	51.5^a	49.5^a	50.2^a	49.8^a
$K_1 \times 10^{-2}$(day^{-1})	2.74E-2	8	3.07	2.74	3.24	3.4	4.46	5.04
$K_2 \times 10^{-4}$(day^{-1})	2E-2	5.24	1.87	1.75	1.78	2.25	1.25	2.32
$K_3 \times 10^{-6}$(day^{-1})	2E-1	9.24	4.72^a	4.72^a	4.71^a	4.71^a	4.74^a	4.73^a
$1/K_1$ (day)	–	–	32.6	36.5	30.9	29.4	22.4	19.8
$1/K_2$ (year)	–	–	14.7	15.7	15.4	12.2	21.9	11.8
$1/K_2$ (year)	–	–	580.5	580.5	581.7	581.7	578.0	579.2

MC: millet cropland, EG: enclosed grassland, A_i: C pool allocation coefficients (%), K_i: C pool turnover rate (day^{-1}), ^{a} Mean value, parameter ranges estimated according to Sch & del et al. (2013), Weng et al. (2011), Zhou et al. (2010) and Xu et al. (2006).

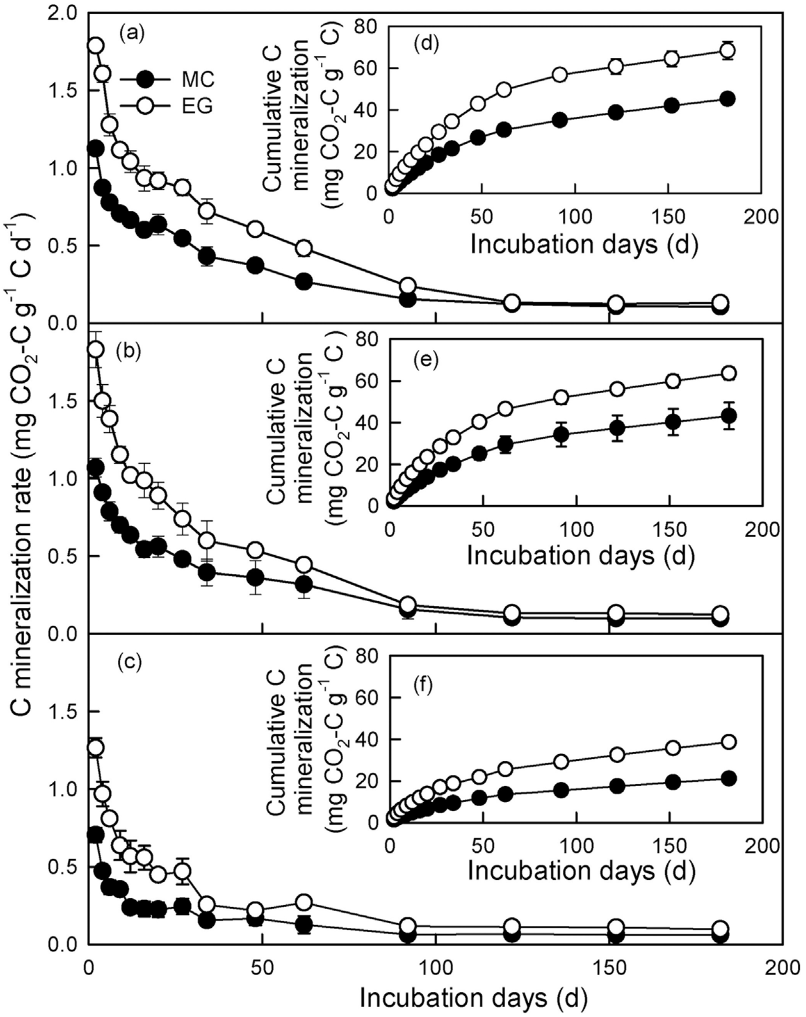

Fig. 1. Soil organic carbon (SOC) mineralization rates (a–c) and cumulative SOC mineralized (d–f) over the whole incubation period at three depths: 0–10 cm (a and d), 10–20 cm (b and e) and 20–30 cm (c and f) for millet cropland (MC, closed circles) and enclosed grassland (EG, open circles). Error bars indicate standard errors.

between MC and EG in the same soil layer. The significant difference was set at $p < 0.05$. Pearson correlation analysis were used to test the relationships between the modeled and observed cumulative SOC mineralized.

3. Results

3.1. Carbon mineralization

Our results showed that the temporal patterns of SOC mineralization were similar for both land use types (Fig. 1). A rapid carbon mineralization rate occurred during the first 92 days for all land use types, and followed by a steady and slow carbon mineralization rate in the next 90 days. The C mineralization rates during the first 92 days were significantly faster in EG than those in MC in all three layers ($p < 0.05$). The cumulative C mineralization for 182 days incubation ranged from 38.6 to 68.4 mg CO_2-C g^{-1}C in EG and from 21.1 to 45.3 mg CO_2-C g^{-1}C in MC (Fig. 1). The cumulative C mineralization in EG were 51%, 47% and 83% greater than those in MC in the 0–10 cm, 10–20 cm and 20–30 cm layer, respectively ($p < 0.05$).

3.2. Inverse analysis of soil C dynamics

Data-model comparisons are important to evaluate the validity of the inverse analysis method. The modeled values were closely related to the observed data ($R^2 = 0.998$, Fig. 2) for both sites. According to the shape of the posterior PDFs, parameters A_1, K_1 and K_2 were well constrained within their *prior* ranges, and parameters A_2 and K_3 were poorly constrained (Fig. 3). The MLEs were calculated for the well constrained parameters, while mean values were calculated for the poorly constrained parameters.

Differences in allocation coefficient and residence times were found between MC and EG (Table 2). The average labile, slow and passive C pool for all soil depths accounted for 2.13%, 50.7% and 47.2% in MC, respectively, and for 3.76%, 49.7% and 46.6% in EG, respectively. The percentage of labile C pool increased after the conversion of cropland into grassland, while the percentage of slow and passive C pool decreased (Table 2). The average residence times of labile, slow and passive organic carbon pool for all soil depths were 28.33 days, 17.33 years and 580 years in MC, respectively, and 28.57 days, 13.23 years and 580 years in EG, respectively. Carbon in labile and slow pools had longer residence times in EG than that in MC in 0–10 cm layer, while the opposite trends were observed in the10-20 and 20–30 cm layers (Table 2).

3.3. Carbon mineralization of different carbon pool

The amounts of active C pool mineralized were 0.11–0.46 mg CO_2-C g^{-1} soil in EG and 0.10–0.21 mg CO_2-C g^{-1} soil in MC. The amount of slow C pool mineralized was 0.12–0.13 mg CO_2-C g^{-1} soil in EG and 0.10–0.12 mg CO_2-C g^{-1} soil in MC, and the cumulative passive C pool was consistently low during the whole incubation period (Fig. 4). The cumulative active and slow C pool mineralized were higher in EG than that in MC (Fig. 4). The labile C pool contributed for 92% in EG and 89% in MC to the C mineralization rate at the beginning of the incubation study. After 92 days, the contribution of the slow C pool to the

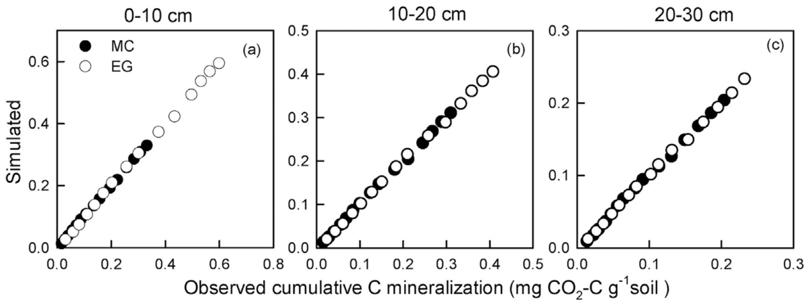

Fig. 2. Correlation between observed cumulative soil organic carbon (SOC) mineralized against simulated cumulative SOC mineralized at three depths: 0–10 cm (a), 10–20 cm (b) and 20–30 cm (c) for millet cropland (MC, closed circles) and enclosed grassland (EG, open circles).

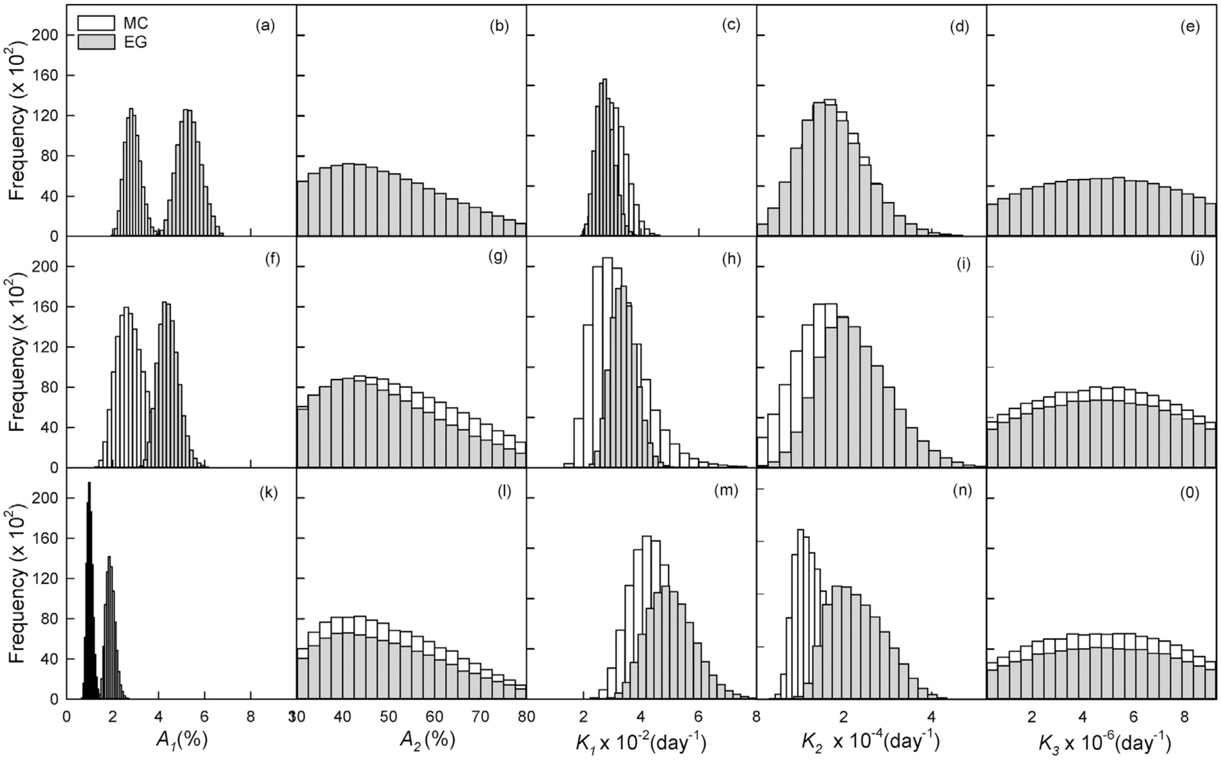

Fig. 3. Frequency distribution of the posterior probability density distribution of the five parameters at three depths: 0–10 cm (a–e), 10–20 cm (f–j) and 20–30 cm (k–o) for millet cropland (MC) and enclosed grassland (EG). A_i: C pool allocation coefficients, K_i: C pool turnover rate.

C mineralization rate was 52% for EG and 60% for MC. The passive C pool only contributed about 2% at the end of the incubation study (Table 3). The results indicated that the active C pool dominated C mineralization for the first 92 days, while the contribution of the slow C pool was the largest after 92 days.

3.4. Different C pool dynamics

At the beginning of the incubation study, the active C pool was 0.10–0.44 mg g^{-1} in EG and 0.09–0.20 mg g^{-1} in MC, the slow C pool was 2.99–4.35 mg g^{-1} in EG and 3.69–4.85 mg g^{-1} in MC, and the passive C pool was 2.90–3.93 mg g^{-1} in EG and 3.27–4.69 mg g^{-1} in MC (Fig. 5). The active C pool from EG plot was larger than that from MC plot. Compared to that in MC, the active C pool declined faster in EG. The slow and passive C pools were higher in EG at the 0–10 cm layer and were lower in EG at the 10–30 cm layer, compared with those in MC. After day 92, active C pool decreased to almost zero for the rest of the incubation. Only about 3% slow C pool was respired at the end of incubation. There was almost no change in passive C pool. After 182 days incubation, total SOC declined about 2.1–4.5% in MC and 3.9–6.8% in EG.

4. Discussion

Although strictly separating C pools with different residence times is challenging (Schädel et al., 2013), it is important to resolve this issue, as the size and turnover times of different C pools have been shown to respond differently to environmental conditions and land use changes (Iqbal et al., 2009). Soil incubation studies can provide a useful way to assess decomposition rates of different C pools, as there is no new input of organic C during the incubation study (Schädel et al., 2013). Furthermore, when soil incubation studies last longer than 100 days, the more recalcitrant C pools will contribute to soil CO_2 efflux and the labile C pool will be eventually depleted (von Lützow and Koegel-Knabner, 2009). Applying the Bayesian inversion approach to optimize parameter estimation can precisely and simply evaluate the different C fraction sizes and turnover times based on the information contained in the time-series data from laboratory incubation experiments (Liang et al., 2015; Schädel et al., 2013, 2014).

In our study, three out of five parameters were well constrained (A_1, K_1 and K_2), while parameters A_2 and K_3 were poorly constrained. Similar to our studies, Sch & del et al. (2013) found that the turnover rates of passive pool were not well constrained from a 385 days incubation experiment. Generally, parameters in relation to fast cycling C processes, such as foliage and fine roots pools, are well constrained, as

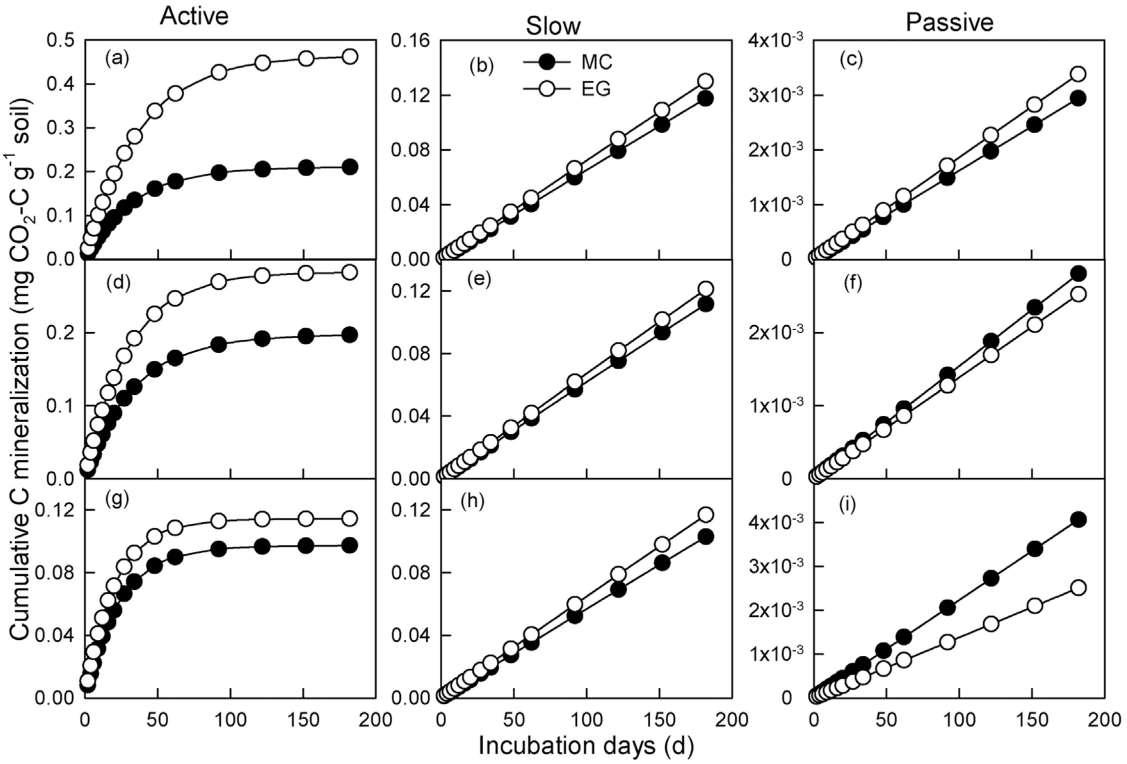

Fig. 4. Cumulative soil organic carbon (SOC) mineralized of active (a, d and g), slow (b, e and h) and passive (c, f and i) carbon pool at three depths: 0–10 cm (a–c), 10–20 cm (d–f) and 20–30 cm (g–i) for millet cropland (MC, closed circles) and enclosed grassland (EG, open circles).

Table 3
Contribution (%) of each C pool to the total respiration rate for the both soil types on average of three soil layers.

	millet cropland			enclosed grassland		
Days	A_1C	A_2C	A_3C	A_1C	A_2C	A_3C
2	89.2	10.5	0.3	92.1	7.7	0.2
4	88.5	11.2	0.3	91.5	8.3	0.2
6	87.7	11.9	0.4	90.8	9.0	0.2
9	86.6	13.0	0.4	90.0	9.8	0.2
12	85.4	14.2	0.4	88.9	10.9	0.2
16	83.7	15.9	0.5	87.3	12.4	0.3
20	81.7	17.7	0.6	85.7	14.0	0.3
27	78.6	20.8	0.6	82.9	16.7	0.4
34	74.1	25.1	0.8	78.8	20.7	0.5
48	67.0	32.0	1.0	71.9	27.5	0.6
62	56.3	42.4	1.3	61.8	37.3	0.8
92	40.3	57.9	1.8	46.4	52.4	1.2
122	22.4	75.3	2.3	28.3	70.1	1.6
152	11.5	85.9	2.6	15.5	82.6	1.9
182	5.5	91.7	2.8	7.8	90.1	2.1

A_iC: specific C pool; contribution of each C pool to the total respiration rate (r) was calculated by $r = h_i^t/h_{total}^t$, where h_i^t is the respiration rate of ith pool at time t, and h_{total}^t is the total respiration rate at time t.

has been reported in other studies (Weng et al., 2011; Zhang et al., 2010). Limited data for calibration is a crucial factor for the poorly constrained parameters (Weng et al., 2011). Carbon fluxes were mainly attributed to active constituents of SOC at the beginning of the experiment and to slow fractions of SOC in the latter phase. The passive fractions of SOC only contributed 2% to the total C efflux. The decomposition rate of passive C pool was very slow. When we applied the parameters into model to simulate the dynamics of SOC pool over 4 years, the passive fractions of SOC mineralized only accounted for less than 3%.

Land-use change affects the physical, chemical and biological properties of soil, influences the quantity and quality of C input (Raiesi and Beheshti, 2014; Sharifi et al., 2013), and thus result in various conditions for the microbial activity. This could be a possible reason for different values of mineralized C. C mineralization rates and the amount of C mineralized during incubation were higher in EG plots in comparison to those in MC plots at all soil depths (Fig. 1). The reduction in SOC mineralization in cropland demonstrated lower microbial activity due to the decline in C availability as a result of the low labile C fraction following cultivation of grassland soils (Raiesi and Beheshti, 2014). This was in agreement with our results where the amount of SOC mineralized was positively correlated to the LF-SOC ($R^2 = 0.98$, $p < 0.01$) and the active C pool of modeling ($R^2 = 0.99$, $p < 0.01$).

Physical and chemical fractionation methods can be used to separate SOC into functionally different pools, while those pools are not homogenous in residence time (Schädel et al., 2013). In contrast, SOC has been divided into multi-C-pool with different residence time in most models of C cycling. Inverse analysis can extract information contained in incubation data, and can determine C pool allocation with different residence time (Schädel et al., 2013). In our study, inverse analysis clearly showed that the active C pool and its percentage in MC plots (0.99%–2.8%) was less than that in EG plots (1.85%–5.17%) at all soil depths (Table 2), which was in agreement with the results of our experimental study. The lower LF-SOC was observed in MC in comparison with EG (Table 1). Since active C pool is labile, a small change in the global pool size can result in an apparent change in atmospheric CO2 concentration and result in a rapid impact on the global climate (Yang et al., 2007). In the surface layer, tillage may expose physical protection labile or fresh organic C to microbial decomposition as a result of destruction of soil structure (Guo and Gifford, 2002; Li et al., 2007; Sharifi et al., 2013), which would result in rapid depletion of labile C fraction and the accumulation of recalcitrant fraction of SOC (Qiao et al., 2015; Raiesi and Beheshti, 2014). Ploughing activities also could reduce soil bulk density thereby increasing soil porosity, promoting soil aeration, which may accelerate loss of SOC through microbial mineralization (Barral et al., 2007; Raiesi and Beheshti, 2014). Additionally, the decreases in the sizes of active C pool in the cropland

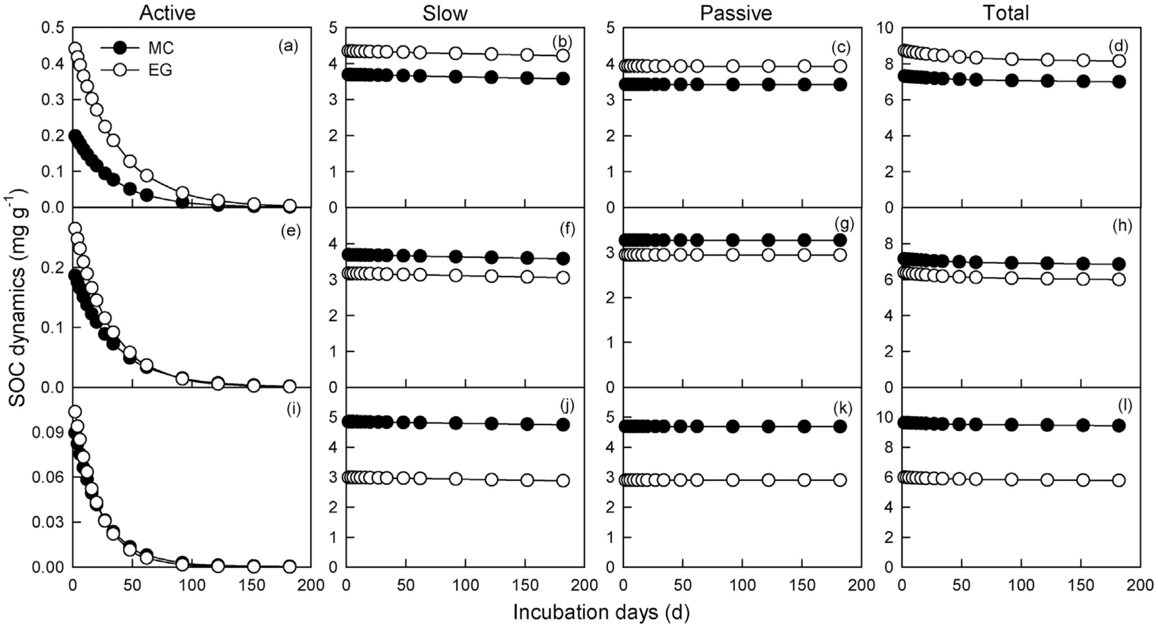

Fig. 5. Soil organic carbon pool (SOC) dynamics over the incubation period at three depths: 0–10 cm (a–c), 10–20 cm (d–f) and 20–30 cm (g–i) for millet cropland (MC, closed circles) and enclosed grassland (EG, open circles). a, e and i active C pool, b, f and j slow C pool, c, g and k passive C pool, d, h and l total SOC pool.

might be attributed to the low inputs of plant residues to the soil, which reduced the fractions of easily decomposable C (Jha et al., 2012a; Raiesi and Beheshti, 2014) and, consequently, decreased SOC mineralization. In this area, most of the crop residues including above- and belowground parts were removed from the soil because of the special harvest method, and thereby reduced the return of C to the soil (Guo et al., 2013; Li et al., 2008). Therefore, significant decreases in soil active C pool in cropland could be attributed to the combined influences of lower organic C inputs and plough activities.

In the 0–10 cm layer, the turnover of the active and slow C pool was slower in EG plots than that in MC plots, while the opposite was observed in the 10–30 cm layers. The results, consistent with our hypothesis, could partly explain why SOC decreases in EG plots in the subsurface layers. The faster turnover rates of slow C pools in the 10–30 cm layers might be attributed to the higher C inputs in EG plots than that in MC plots (Guo et al., 2013). It has been suggested that the increase of C inputs to soils through plant litter can stimulate microbial respiration enough to outpace the increased C inputs to soil, which consequently resulted in a reduction in soil C (Langley et al., 2009). Previous work also showed that the increase of the distribution of fresh C at depth could stimulate the decline in ancient C (Fontaine et al., 2007). Although microorganisms can decompose ancient C in subsoil of cropland, the energy from substrate was not sufficient to support long-term biological activity due to the lack of fresh C. Chronic fertilizer additions may also result in reducing fungal biomass and activity and lignin accumulation, consequently, resulted in a suppression of organic matter decomposition and SOC accumulation (Frey et al., 2014). Moreover, the addition of nutrients could increase net humification efficiency, and sequester C into the more stable fine fraction pool of soil organic matter (Kirkby et al., 2013). As a result, SOC was higher and the residence time was longer in cropland compared to those in grassland in subsurface soil. Probably, in surface layer, increased soil aeration by tillage and reduction in physical protection of organic C due to cultivation might have contributed to short residence time in cropland.

The active C pool comprised 0.99%–5.20% of total SOC in the two land use types. The data was in a similar range with that found by Lim et al. (2012), who reported that active C pool comprised 0.5%–9.5% of total SOC. The residence times of active C pool varied from 19.8 to 36.5 days, which was in agreement with previous studies conducted by Qian et al. (2013) and Yang et al. (2007), but lower than that (2–10 months) estimated by Zhang et al. (2010). Since incubation study was often performed under optimal temperature and moisture conditions, that the residence times of SOC in the field may be longer than those in incubation studies (Schädel et al., 2013). Carbon residence times of 11.8–21.9 years in slow C pools in our study were similar to the studies by Iqbal et al. (2009) and Jha et al. (2012a). The residence times of the passive C pool could not be exactly determined as the parameter was poorly constrained.

Inverse analysis can not only estimate the sizes and turnover times of different C pools based on dynamic characteristics in soil CO_2 flux data from incubation studies, but also determines the dynamics of different C pools over the whole incubation study (Schädel et al., 2013). According to inverse analysis, the contribution of active C pool dominated the CO_2 efflux up to 90% at the beginning of the incubation, while the slow C pool was dominating the CO_2 efflux after 92 days (Table 3). The dynamics of contribution of each C pool to total respiration rate was consistent with the pattern of soil C mineralization rates which was fast during the first 92 days thereafter slow down and kept relatively stable in the next 90 days (Fig. 1). This reflected a change from labile to recalcitrant C and has been illustrated in previous studies (Jha et al., 2012a, 2012b; Wang et al., 2013). The rapid rate of C mineralization during the early stages of incubation was mainly resulted from the decomposition of the labile C pool (such as sugars and starches), and the decrease in C mineralization rate at the later stage was probably due to the rising proportion of recalcitrant C pool (such as lignin and cellulose) and the loss of labile C pool (Jha et al., 2012a, 2012b). The fraction of total carbon (between 2.1% and 6.8% of the initial SOC) that respired after 182 days incubation was very low in all cases. Although the result was lower than those found by some researchers (Sch & del et al., 2013; Weintraub and Schimel, 2003) and they were in agreement with those reported by Rey and Jarvis (2006), who showed that 2% ~ 10% of the initial SOC was released after 270 days of incubation. This indicated that most of the SOC was in the recalcitrant fraction at our study sites. Previous studies have also found that more than 85% SOC was in the recalcitrant form and was the difficultly decomposed component of SOC (i.e. heavy fraction organic C) (Han et al., 2015).

Inverse analysis of incubation studies can determine the size and residence time of different C pool and is a powerful technique to accurately estimate SOC dynamics. The C dynamics of soil incubations with different treatment, soil types and vegetation can be analyzed when using the inverse analysis approach. This modeling approach can detect even small changes between soils (Schädel et al., 2013). Applying the Bayesian inversion approach can precisely and simply evaluate the different C fraction sizes and turnover times, which can be applied into ecosystem models and improve understanding of soil C cycling. Our results clearly showed that land use conversion from cropland to grassland resulted in being increased rates of SOC mineralization and cumulative SOC mineralized due to the increase in the substrate quality (LF-SOC). Inverse analysis also showed that active C pool was greater in grassland than in cropland. Low C input and ploughing activities were the dominant driving factors decreasing active C pool in cropland. The modeling results supported our hypothesis that, the residence times of slow C pool were shorter in grassland in comparison to cropland, which could partly explain the diminished SOC in subsoil in grassland. In addition, inverse analysis could directly give an insight that SOC mineralization was mainly resulted from the labile C pool during the early stages of incubation and from the resistant C pool at the later stage. Further research is needed to understand the change of C residence times as time goes after conversion of cropland into grassland.

Acknowledgements

We thank anonymous reviewers for their valuable suggestions and the Semi-Arid Climate and Environment Observatory of Lanzhou University for providing useful information. This study was funded by the National Key R & D Program of China (2016YFC0500505), Natural Science Foundation of China (31502010; 31201838; 31602001), Open Project Program of State Key Laboratory of Grassland Agro-ecosystems (SKLGAE201401), Fundamental Research Funds for the Central Universities (lzujbky-2016-13), Key scientific and technological projects of Xinjiang (2016A03006-1) and the 111 project (B120002).

References

Alef, K., 1995. Soil respiration. In: Alef, K.P.N. (Ed.), Methods in Applied Soil Microbiology and Biochemistry. Acadamic Press, London, pp. 214–222.

Andren, O., Paustian, K., 1987. Barley straw decomposition in the field − a comparison of models. Ecology 68, 1190–1200.

Barral, M.T., Bujan, E., Devesa, R., Iglesias, M.L., Velasco-Molina, M., 2007. Comparison of the structural stability of pasture and cultivated soils. Sci. Total Environ. 378, 174–178.

Bremner, J., 1996. Nitrogen-total. In: Sparks, D., Page, A., Helmke, P., Loeppert, R., Soltanpour, P., Tabatabai, M., Johnston, C., Sumner, M. (Eds.), Methods of Soil Analysis. Part 3-chemical Methods. Soil Science Society of America Madison, WI, pp. 1085–1121.

Chang, R.Y., Fu, B.J., Liu, G.H., Liu, S.G., 2011. Soil carbon sequestration potential for grain for green project in loess plateau. China. Environ. Manage. 48, 1158–1172.

Chen, S.T., Huang, Y., Zou, J.W., Shi, Y.S., 2013. Mean residence time of global topsoil organic carbon depends on temperature, precipitation and soil nitrogen. Global Planet. Change 100, 99–108.

Davidson, E.A., Janssens, I.A., 2006. Temperature sensitivity of soil carbon decomposition and feedbacks to climate change. Nature 440, 165–173.

Derrien, D., Amelung, W., 2011. Computing the mean residence time of soil carbon fractions using stable isotopes: impacts of the model framework. Eur. J. Soil Sci. 62, 237–252.

Feng, X., Fu, B., Lu, N., Zeng, Y., Wu, B., 2013. How ecological restoration alters ecosystem services: an analysis of carbon sequestration in China's Loess Plateau. Sci. Rep. 3.

Fontaine, S., Barot, S., Barré, P., Bdioui, N., Mary, B., Rumpel, C., 2007. Stability of organic carbon in deep soil layers controlled by fresh carbon supply. Nature 450, 277–280.

Fröberg, M., Tipping, E., Stendahl, J., Clarke, N., Bryant, C., 2011. Mean residence time of O horizon carbon along a climatic gradient in Scandinavia estimated by 14C measurements of archived soils. Biogeochemistry 104, 227–236.

Frey, S.D., Ollinger, S., Nadelhoffer, K., Bowden, R., Brzostek, E., Burton, A., Caldwell, B.A., Crow, S., Goodale, C.L., Grandy, A.S., Finzi, A.C., Kramer, M.G., Lajtha, K., LeMoine, J., Martin, M., McDowell, W.H., Minocha, R., Sadowsky, J.J., Templer, P.H., Wickings, K., 2014. Chronic nitrogen additions suppress decomposition and sequester soil carbon in temperate forests. Biogeochemistry 121, 305–316.

Friend, A.D., Lucht, W., Rademacher, T.T., Keribin, R., Betts, R., Cadule, P., Ciais, P., Clark, D.B., Dankers, R., Falloon, P.D., Ito, A., Kahana, R., Kleidon, A., Lomas, M.R., Nishina, K., Ostberg, S., Pavlick, R., Peylin, P., Schaphoff, S., Vuichard, N., Warszawski, L., Wiltshire, A., Woodward, F.I., 2014. Carbon residence time dominates uncertainty in terrestrial vegetation responses to future climate and atmospheric CO2. Proc. Natl. Acad. Sci. U. S. A. 111, 3280–3285.

Fu, B.J., Zhao, W.W., Chen, L.D., Zhang, Q.J., Lu, Y.H., Gulinck, H., Poesen, J., 2005. Assessment of soil erosion at large watershed scale using RUSLE and GIS: A case study in the Loess Plateau of China. Land Degrad. Dev. 16, 73–85.

Gelman, A., Rubin, D.B., 1992. Inference from iterative simulation using multiple sequences. Stat. Sci. 7, 457–472.

Gregorich, E., Ellert, B., 1993. Light fraction and macroorganic matter in mineral soils. In: Carter, M.R., Gregorich, E. (Eds.), Soil Sampling and Methods of Analysis. Canadian Society of Soil Science, Lewis Boca Raton, pp. 397–407.

Guo, L.B., Gifford, R.M., 2002. Soil carbon stocks and land use change: a meta analysis. Global Change Biol. 8, 345–360.

Guo, D., Li, X., Li, X., Wang, J., Fu, H., 2013. Conventional tillage increases soil microbial biomass and activity in the Loess Plateau, China. Acta Agric. Scand. Sect. B-Soil Plant Sci. 63, 489–496.

Han, H.G., Li, X.D., Niu, D.C., Hall, S.J., Guo, D., Wan, C.G., Learned, J.K., Fu, H., 2015. Conventional tillage improves the storage of soil organic carbon in heavy fractions in the Loess Plateau, China. J. Arid Land 7, 636–643.

Hastings, W.K., 1970. Monte Carlo sampling methods using Markov chains and their applications. Biometrika 57, 97–109.

Iqbal, J., Hu, R.G., Lin, S., Ahamadou, B., Feng, M.L., 2009. Carbon dioxide emissions from Ultisol under different land uses in mid-subtropical China. Geoderma 152, 63–73.

Jha, P., De, A., Lakaria, B.L., Biswas, A.K., Singh, M., Reddy, K.S., Rao, A.S., 2012a. Soil carbon pools, mineralization and fluxes associated with land use change in vertisols of central India. Natl. Acad. Sci. Lett.-India 35, 475–483.

Jha, P., Garg, N., Lakaria, B.L., Biswas, A.K., Rao, A.S., 2012b. Soil and residue carbon mineralization as affected by soil aggregate size. Soil Tillage Res. 121, 57–62.

Kirkby, C.A., Richardson, A.E., Wade, L.J., Batten, G.D., Blanchard, C., Kirkegaard, J.A., 2013. Carbon-nutrient stoichiometry to increase soil carbon sequestration. Soil Biol. Biochem. 60, 77–86.

Lü, Y.H., Fu, B.J., Feng, X.M., Zeng, Y., Liu, Y., Chang, R.Y., Sun, G., Wu, B.F., 2012. A policy-driven large scale ecological restoration: quantifying ecosystem services changes in the Loess plateau of China. PLoS One 7.

Langley, J.A., McKinley, D.C., Wolf, A.A., Hungate, B.A., Drake, B.G., Megonigal, J.P., 2009. Priming depletes soil carbon and releases nitrogen in a scrub-oak ecosystem exposed to elevated CO2. Soil Biol. Biochem. 41, 54–60.

Lee, K.H., Jose, S., 2003. Soil respiration and microbial biomass in a pecan − cotton alley cropping system in Southern USA. Agrofor. Syst. 58, 45–54.

Li, X.G., Wang, Z.F., Ma, Q.F., Li, F.M., 2007. Crop cultivation and intensive grazing affect organic C pools and aggregate stability in and grassland soil. Soil Tillage Res. 95, 172–181.

Li, X., Fu, H., Li, X., Guo, D., Dong, X., Wan, C., 2008. Effects of land-use regimes on carbon sequestration in the Loess Plateau, northern China. N. Z. J. Agric. Res. 51, 45–52.

Li, X.D., Fu, H., Guo, D., Li, X.D., Wan, C.G., 2010. Partitioning soil respiration and assessing the carbon balance in a Setaria italica (L.) Beauv. Cropland on the Loess Plateau, Northern China. Soil Biol. Biochem. 42, 337–346.

Liang, J.Y., Li, D.J., Shi, Z., Tiedje, J.M., Zhou, J.Z., Schuur, E.A.G., Konstantinidis, K.T., Luo, Y.Q., 2015. Methods for estimating temperature sensitivity of soil organic matter based on incubation data: a comparative evaluation. Soil Biol. Biochem. 80, 127–135.

Lim, S.S., Lee, K.S., Lee, S.I., Lee, D.S., Kwak, J.H., Hao, X.Y., Ro, H.M., Choi, W.J., 2012. Carbon mineralization and retention of livestock manure composts with different substrate qualities in three soils. J. Soils Sediments 12, 312–322.

Lu, C.H., van Ittersumb, M.K., Rabbinge, R., 2004. A scenario exploration of strategic land use options for the Loess Plateau in northern China. Agric. Syst. 79, 145–170.

Luo, Y.Q., White, L.W., Canadell, J.G., DeLucia, E.H., Ellsworth, D.S., Finzi, A.C., Lichter, J., Schlesinger, W.H., 2003. Sustainability of terrestrial carbon sequestration: a case study in Duke forest with inversion approach. Global Biogeochem. Cycles 17.

Luo, Y.Q., Weng, E.S., Wu, X.W., Gao, C., Zhou, X.H., Zhang, L., 2009. Parameter identifiability, constraint, and equifinality in data assimilation with ecosystem models. Ecol. Appl. 19, 571–574.

Ma, L., Guo, C., Xin, X., Yuan, S., Wang, R., 2013. Effects of belowground litter addition, increased precipitation and clipping on soil carbon and nitrogen mineralization in a temperate steppe. Biogeosciences 10, 7361–7372.

Metropolis, N., Rosenbluth, A.W., Rosenbluth, M.N., Teller, A.H., Teller, E., 1953. Equation of state calculations by fast computing machines. J. Chem. Phys. 21, 1087.

Mohanty, S., Nayak, A.K., Kumar, A., Tripathi, R., Shahid, M., Bhattacharyya, P., Raja, R., Panda, B.B., 2013. Carbon and nitrogen mineralization kinetics in soil of rice–rice system under long term application of chemical fertilizers and farmyard manure. Eur. J. Soil Biol. 58, 113–121.

Nelson, D.W., Sommers, L.E., 1996. Total carbon, organic carbon, and organic matter. In: Sparks, D., Page, A., Helmke, P., Loeppert, R., Soltanpour, P., Tabatabai, M., Johnston, C., Sumner, M. (Eds.), Methods of Soil Analysis. Part 3-Chemical Methods. Soil Science Society of America Madison, WI, pp. 961–1010.

Parton, W.J., Schimel, D.S., Cole, C., Ojima, D., 1987. Analysis of factors controlling soil organic matter levels in Great Plains grasslands. Soil Sci. Soc. Am. J. 51, 1173–1179.

Parton, W.J., Stewart, J.W., Cole, C.V., 1988. Dynamics of C, N, P and S in grassland soils: a model. Biogeochemistry 5, 109–131.

Qian, H.Y., Pan, J.J., Sun, B., 2013. The relative impact of land use and soil properties on sizes and turnover rates of soil organic carbon pools in Subtropical China. Soil Use Manag. 29, 510–518.

Qiao, N., Xu, X.L., Cao, G.M., Ouyang, H., Kuzyakov, Y., 2015. Land use change decreases soil carbon stocks in Tibetan grasslands. Plant Soil 395, 231–241.

Raiesi, F., Beheshti, A., 2014. Soil C turnover, microbial biomass and respiration, and enzymatic activities following rangeland conversion to wheat-alfalfa cropping in a semi-arid climate. Environ. Earth Sci. 72, 5073–5088.

Raupach, M., Rayner, P., Barrett, D., DeFries, R., Heimann, M., Ojima, D., Quegan, S., Schmullius, C., 2005. Model?data synthesis in terrestrial carbon observation: methods, data requirements and data uncertainty specifications. Global Change Biol. 11, 378–397.

Rey, A., Jarvis, P., 2006. Modelling the effect of temperature on carbon mineralization rates across a network of European forest sites (FORCAST). Global Change Biol. 12, 1894–1908.

Richards, A.E., Dalal, R.C., Schmidt, S., 2007. Soil carbon turnover and sequestration in native subtropical tree plantations. Soil Biol. Biochem. 39, 2078–2090.

Saggar, S., Parshotam, A., Sparling, G.P., Feltham, C.W., Hart, P.B.S., 1996. C-14-labelled ryegrass turnover and residence times in soils varying in clay content and mineralogy. Soil Biol. Biochem. 28, 1677–1686.

Schädel, C., Luo, Y., Evans, R.D., Fei, S., Schaeffer, S.M., 2013. Separating soil CO_2 efflux into C-pool-specific decay rates via inverse analysis of soil incubation data. Oecologia 1–12.

Schädel, C., Schuur, E.A., Bracho, R., Elberling, B., Knoblauch, C., Lee, H., Luo, Y., Shaver, G.R., Turetsky, M.R., 2014. Circumpolar assessment of permafrost C quality and its vulnerability over time using long-term incubation data. Global Change Biol. 20, 641–652.

Sharifi, M., Zebarth, B.J., Burton, D.L., Drury, C.F., Grant, C.A., 2013. Mineralization of carbon-14-labeled plant residues in conventional tillage and no-till systems. Soil Sci. Soc. Am. J. 77, 123–132.

Trumbore, S.E., 1997. Potential responses of soil organic carbon to global environmental change. Proc. Natl. Acad. Sci. U. S. A. 94, 8284–8291.

Trumbore, S., 2000. Age of soil organic matter and soil respiration: radiocarbon constraints on belowground C dynamics. Ecol. Appl. 10, 399–411.

Vogt, K.A., Vogt, D.J., Palmiotto, P.A., Boon, P., O'Hara, J., Asbjornsen, H., 1996. Review of root dynamics in forest ecosystems grouped by climate, climatic forest type and species. Plant Soil 187, 159–219.

Wang, G.B., Zhou, Y., Xu, X., Ruan, H.H., Wang, J.S., 2013. Temperature sensitivity of soil organic carbon mineralization along an elevation gradient in the wuyi mountains, China. PLoS One 8.

Weintraub, M.N., Schimel, J.P., 2003. Interactions between carbon and nitrogen mineralization and soil organic matter chemistry in arctic tundra soils. Ecosystems 6, 129–143.

Weng, E.S., Luo, Y.Q., Gao, C., Oren, R., 2011. Uncertainty analysis of forest carbon sink forecast with varying measurement errors: a data assimilation approach. J. Plant Ecol.-Uk 4, 178–191.

Xu, T., White, L., Hui, D.F., Luo, Y.Q., 2006. Probabilistic inversion of a terrestrial ecosystem model: analysis of uncertainty in parameter estimation and model prediction. Global Biogeochem. Cycles 20, 1–15.

Yang, L., Pan, J., Shao, Y., Chen, J.M., Ju, W.M., Shi, X., Yuan, S., 2007. Soil organic carbon decomposition and carbon pools in temperate and sub-tropical forests in China. J. Environ. Manage. 85, 690–695.

Zhang, L., Luo, Y.Q., Yu, G.R., Zhang, L.M., 2010. Estimated carbon residence times in three forest ecosystems of eastern China: applications of probabilistic inversion. J. Geophys. Res.-Biogeosci. 115.

Zhou, X.H., Luo, Y.Q., Gao, C., Verburg, P.S.J., Arnone, J.A., Darrouzet-Nardi, A., Schimel, D.S., 2010. Concurrent and lagged impacts of an anomalously warm year on autotrophic and heterotrophic components of soil respiration: a deconvolution analysis. New Phytol. 187, 184–198.

Zhou, X., Zhou, T., Luo, Y., 2012. Uncertainties in carbon residence time and NPP-driven carbon uptake in terrestrial ecosystems of the conterminous USA: a Bayesian approach. Tellus B 64.

von Lützow, M., Koegel-Knabner, I., 2009. Temperature sensitivity of soil organic matter decomposition-what do we know? Biol. Fertil. Soils 46, 1–15.